Estimation of Q from surface-seismic reflection data in data space and image space

Yi Shen

ABSTRACT

Estimating seismic attenuation, or Q, is crucial for imaging applications, reservoir characterization and seismic acquisition design. A new method for Q estimation uses central frequency shift to analyze Q versus offset or angle in both the data space and image space. Q migration and Q compensation are also presented here for the image-based Q estimation. Applying this new approach to a 2D synthetic model demonstrate that both data-based and image-based methods are able to accurately estimate Q for a model with flat reflectors and homogeneous medium.

INTRODUCTION

Seismic waves propagating through the earth are attenuated by intrinsic attenuation and scattering attenuation. Scattering attenuation transfers wave energy to later arrivals or other directions. Intrinsic attenuation transfers wave energy to heat. An understanding of intrinsic attenuation has three major motivations.

First, attenuation is important for characterizing rock and fluid properties, e.g., saturation, porosity, permeability, and viscosity, because attenuation is more sensitive than velocity to some of these properties. For example, Q can serve as a lithology discriminator in a frontier area with sparse well control (Dasgupta and Clark, 1998). In addition, since the magnitude of the attenuation is directly related to petrophysical parameters, Q analysis provides a potential tool for reservoir characterization; it can help determine the contents (e.g. gas saturation) of a reservoir, map fracture azimuth to target reservoir development, and monitor the mobility of reservoir fluids to optimize the injection process.

Second, if ones knew the absorption properties of the subsurface, they could include them in seismic data processing (deconvolution, stacking, migration, inverse Q filtering, etc.) and get sharper images and higher resolutions. Attenuation estimation could also be used to better interpret the effects of AVO and anisotropy, which have offset-dependent signatures. Furthermore, full waveform inversion can achieve improved accuracy by incorporating attenuation into the initial model.

Third, attenuation estimates are useful in seismic acquisition design. Knowing the level of seismic attenuation in the survey-planning stage helps determine how much signal may reach the target, and enables the optimization of acquisition parameters.

However, it is difficult to estimate seismic attenuation. First, it is hard to distinguish intrinsic attenuation and scattering attenuation. In this study, I concentrate on the intrinsic attenuation and try to reduce the influence of the scattering attenuation. In the situation when the scattering attenuation cannot be ignored, the estimated attenuation is a combination of intrinsic and scattering effects. The other most important reason is that amplitudes are easily affected by many factors, such as geometric spreading, source and receiver coupling, radiation patterns, transmission/reflection effects, focusing effects, PS conversion, etc. In this paper, I first review existing methods of estimating Q and illustrate how they account for these contaminating factors. Then, according to the advantages and drawbacks of these conventional Q measurements, I propose a new method of Q estimation from surface seismic data and test it on a 2D synthetic model.

METHODS REVIEW

In this section, I review previous studies which have addressed Q estimation, and discuss how they solve the challenges listed above. Generally, Q tomography algorithms are classified into two main categories. One category is ray-based tomography (Quan and Harris, 1997; Plessix, 2006; Rickett, 2006, 2007), where the relationship between the measurements and the inverse of Q is assumed to be linear. The other category is wave-equation-based tomography (Liao and McMechan, 1996; Hicks and Pratt, 2001; Pratt et al., 2003; Watanabe et al., 2004; Gao et al., 2005; Xin et al., 2008), which is formulated as a nonlinear optimization problem.

Ray-based tomography

In ray-based tomography, the process of wave propagation is described as a linear system, which assumes the relationship between the measurements and the inverse of Q is assumed to be linear. If the amplitude spectrum of an incident wave is $S(f)$ and the instrument/medium response is $G(f)H(f)$, the received amplitude spectrum $R(f)$ may be expressed as

$$R(f) = G(f)H(f)S(f), \tag{1}$$

where the factor $G(f)$ includes geometrical spreading, instrument response, source/receiver coupling, radiation pattern, and reflection/transmission coefficients, and $H(f)$ describes the attenuation effect on the amplitude. Always, $G(f)$ is set to be constant over frequency, because these amplitude factors are frequency independent in the homogeneous media.

Based on this linear assumption, there are several ways of estimating the effective Q. The most popular way is the spectral ratio method. This method takes the

logarithm of equation 1, which is shown as follows:

$$Y(f) = Cf + B, \tag{2}$$

where

$$Y(f) = \ln\left[S(f)/R(f)\right], \tag{3}$$

$$C = \int_{ray} \alpha_0 dl, \tag{4}$$

$$B = -\ln(G), \tag{5}$$

$$\alpha_0 = \frac{\pi}{Qv}. \tag{6}$$

It can be seen that the integrated attenuation C is the slope of the plot of $Y(f)$ versus frequency f. This method may remove the effect of factor G, when G does not depend on frequency f.

The other way of estimating Q is by central frequency shift, which is a statistics-based method that estimates the attenuation coefficient from the spectral centroid downshift over a range of frequencies. In most natural materials, seismic attenuation increases with frequency. The high-frequency components of the seismic signal are attenuated more rapidly than the low-frequency components. As a result, the centroid of the signal's spectrum experiences a downshift during propagation. Under the assumption of a frequency-independent Q model, this downshift is proportional to a path integral through the attenuation distribution and can be used as observed data to reconstruct the attenuation distribution tomographically. The relation between the downshift and the attenuation is mathematically shown as follows,

$$\int_{ray} \alpha_0 dl = (f_s - f_R)/\sigma_s^2, \tag{7}$$

where the central frequency is defined as $f_c = \frac{\int_0^\infty fS(f)df}{\int_0^\infty S(f)df}$, f_s is the central frequency of the input source, f_R is the central frequency of the received signal, and σ_s is the variance of the source spectrum.

The advantage of these two methods is that they do not depend on amplitude scaling. However, they are not robust and will not work if the signal-to-noise ratio is poor. In addition, these two methods need a reference or source amplitude. Furthermore, since these methods are based on ray tomography, they share the limitations and assumptions of the ray-based method, which has a low computational cost but cannot handle complex structure.

Wave-equation-based method

According to its definition, Q is a function of the real and imaginary velocity components

$$Q = -\frac{v_r}{2v_i}. \tag{8}$$

The wave-equation-based method uses velocity to estimate Q and regards velocity and Q as two variables to be estimated. This method is physically more accurate but is computationally expensive and has trade-offs between the effects on data amplitude of these different parameter classes.

PROPOSED METHOD

I propose a new method that balances the advantages and disadvantages of the conventional methods discussed in the above section. The basic idea of this proposed method is to use central frequency shift (Quan and Harris, 1997) to analyze Q versus offset (QVO) (Dasgupta and Clark, 1998) or Q versus angle (QVA) in the image domain.

According to equation 7, the central frequency shift varies with offset because of differing raypath geometries, and hence in accumulated attenuation. Specifically, if I define a central-frequency versus offset or versus angle domain, the central frequency is flat when there is no absorption, but shows a curvature in an absorptive medium. By the same reasoning, the same response can be observed in the central-wavenumber-versus-offset/angle domain, which can be obtained after migration.

Advantage

Using central freqency shift to analyze QVO/QVA has several advantages over the previous Q estimation methods (Quan and Harris, 1997; Plessix, 2006; Rickett, 2006, 2007), which analyze Q from a stacked trace. First, the spectral amplitude of a stacked trace has a distorted attenuation signature, since the path lengths (hence accumulated attenuation), spectral distortions from NMO stretch, and reflectivity-transmissivity effects vary from one trace to the next for a given reflection event. Performing an analysis along the offset or angle may help reduce such distortion. Second, with the relevant information from different offsets or angles, I do not need the reference/source information that is a prerequisite for the previous methods. Third, a number of applications have already demonstrated the effectiveness of QVO for discrimination of lithology types (Dasgupta and Clark, 1998; Hackert and Parra, 2004), azimuthal discrimination of fractures (Clark et al., 2009; Moffat et al., 2009), and discrimination of time-lapse changes (Clark et al., 2001; Blanchard et al., 2009). In addition, there are also several potentially promising applications for this method. For example, such analysis may reduce the ambiguity between velocity and attenuation, because velocity does not have a frequency-dependent effect on the amplitude, and thus has no central-frequency shift. QVO may also help analyze amplitude variation with offset (AVO), as attenuation effects are always superimposed on AVO signature.

Migration-based Q analysis is used in this proposed method, instead of the ray-based Q estimation methods that were used in previous methods. One advantage of using a migration-based method is that in the presence of complex wave propagation (i.e. multipathing and geometrical dispersion), data-based methods often cannot produce high-quality images, while migration-based methods yield better images because they can handle the complex structure in the subsurface. In addition, the signal-to-noise ratio is higher in the image domain than in the data domain, leading to a higher-quality result from the central-frequency shift.

Challenge

A number of factors make determining the attenuation difficult using this method. First, the difficulty comes from the effects on the seismic spectrum from interference of different seismic arrivals, so it is necessary to carefully window the desired reflector or variable-window time-frequency transform. Second, angle-dependent effects (directivity, anisotropy, raypath differences) hamper accurate interval measurements. Third, geometric information (local velocity, dip event, opening angle) must be taken into consideration in the image domain.

THEORY AND NUMERICAL TESTS

Forward modeling with Q

There are different models to describe Q: the Maxwell model, the Kelvin-Voigt model, the Zener model, the Burgers model, etc. Q behaves differently in the frequency domain in these different models. However, I use a nearly constant-Q model in this paper. The reason is that in oil prospecting and seismology, constant-Q models are convenient to parametrize attenuation in rocks, since the frequency dependence is usually not known. Moreover, there is physical evidence that attenuation is almost linear within the range of seismic frequencies, and thus the effect of Q is independent of these frequencies. Futterman (1962) has developed the theory for nearly constant Q, and I can use it in the forward modeling with Q.

In Futterman's theory, the visco-acoustic equation has the same form as the acoustic equation, but the velocity is a complex number,

$$\tilde{v}(\omega) = v_{\omega r}\left(1 - \frac{1}{\pi Q}\ln(\omega/\omega_r)\right)^{-1}\left(1 + \frac{i}{2Q}\right)^{-1}, \tag{9}$$

where ω_r is the reference angular frequency, and $v_{\omega r}$ is the velocity at the reference angular frequency. Forward modeling can be executed with equation 9 using conventional one-way downward continuation, and more detailed algorithm is described in equations 11-16 in the following migration section.

I present a simple 2D synthetic example for the forward modeling. The model size is 4000 m (length) x 2500 m (depth). A horizontal reflector is at 1500 m depth. The source is located at x=0 on the surface, and 401 receivers are uniformly distributed along the surface. The medium is assumed to be homogeneous with constant velocity (2000 m/s) and constant Q (50 for the model with attenuation and 99999 for the model without attenuation). Injecting a Ricker wavelet produces the forward-modeled data in Figures 1(a) and 1(b). Their central frequencies are shown in Figures 1(c) and 1(d).

The wavelet in Figure 1(a) is stretched relative to the one in Figure 1(b), because the high frequency is attenuated more than the low frequency, which broadens the wavelet. Their central frequencies are also significantly different. Central frequency with attenuation in Figure 1(c) is a hyperbola along the offset, matching the theoretical calculation well. In contract, the central frequency is a flat line in Figure 1(d), indicating that no attenuation is accumulated along the ray path. Hence, Figures 1(c) and 1(d) provide further evidence that QVO carries information about attenuation and can be used to estimate Q.

Estimation of Q from data space

Because this simple 2D example has no complex structure or noise, I apply a data-space QVO method to this model before going to the image domain. According to the theory developed by Quan and Harris (1997), the central-frequency shift changes with attenuation in the way described in equation 7. If the wave travels in the homogeneous media and reflected from one flat reflector, equation 7 can be simplified in the following way,

$$x^2 + z^2 = C^2 \Delta f^2 Q^2, \tag{10}$$

where x is offset, z is depth, $\Delta f = (f_S - f_R)$, and $C = v/(\pi\sigma_S^2)$, which is a constant if I assume the velocity and the variance of the source are known.

Equation 10 relates four variables: two coordinates of the data space $(x, \Delta f)$ and two of the model space $(z, 1/Q)$. An impulse in model space corresponds to a hyperbola in data space. In the opposite case, an impulse at a point in data space corresponds to another hyperbola in the model space. If I sum along the trajectories in the data space, energy will be concentrated in the model space to indicate the Q value. In this paper, I define the model space as the Q-spectra and the procedure described above as the Q-scan. Least-squares inversion can also be used here to yield a better result.

Figure 2(a) shows the central-frequency shift of the modeled data in Figure 1(a). After scanning, I compute the Q-spectra in Figure 2(b). This result shows concentrated energy around the expected point (1500 m, 0.02), which indicates that the RMS Q is 50 above 1500 m depth. Figure 2(c) shows least-squares inversion after 50 iterations. The energy is more focused on the expected point and shows much higher resolution. Therefore, I conclude that computing the Q-spectra can be used

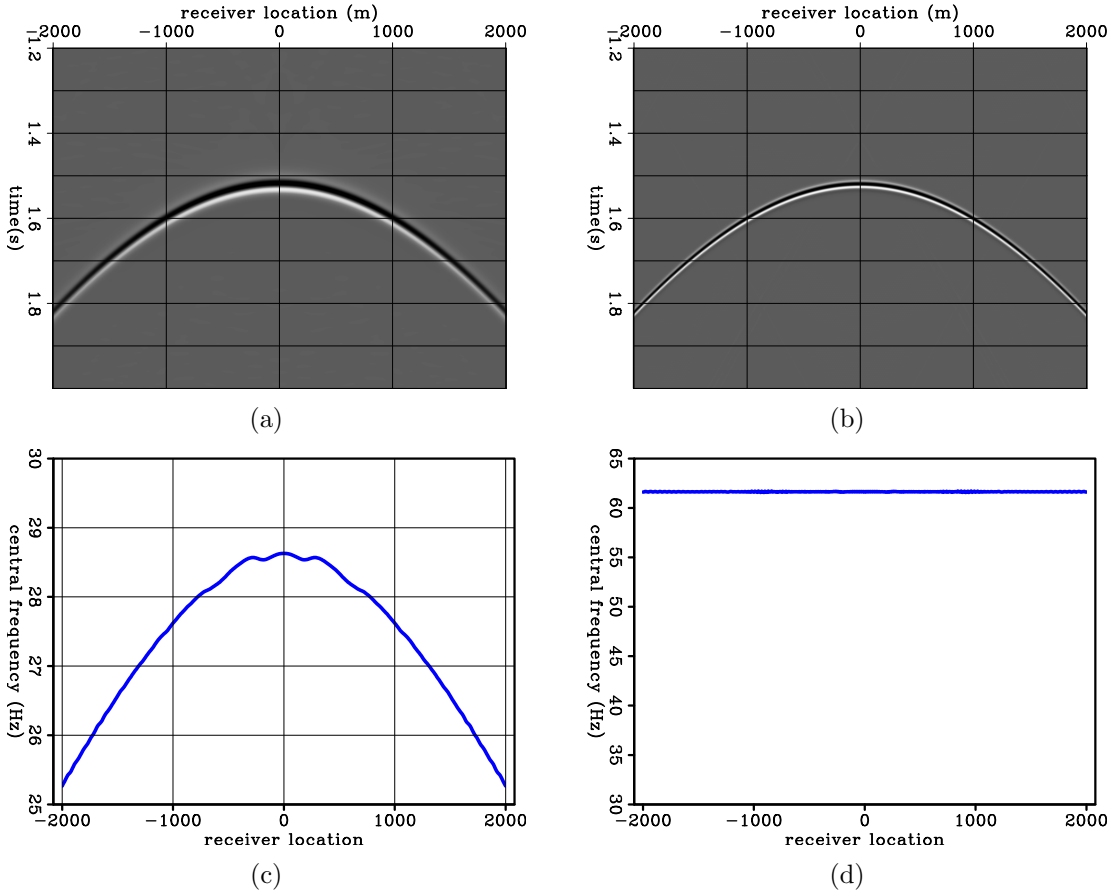

Figure 1: Given the 2D synthetic example, (a) modeled data with attenuation (Q=50); (b) modeled data without attenuation (Q=99999); (c) central frequency with attenuation; (d) central frequency without attenuation. [**ER**]

in estimating the RMS Q for a model with simple structure.

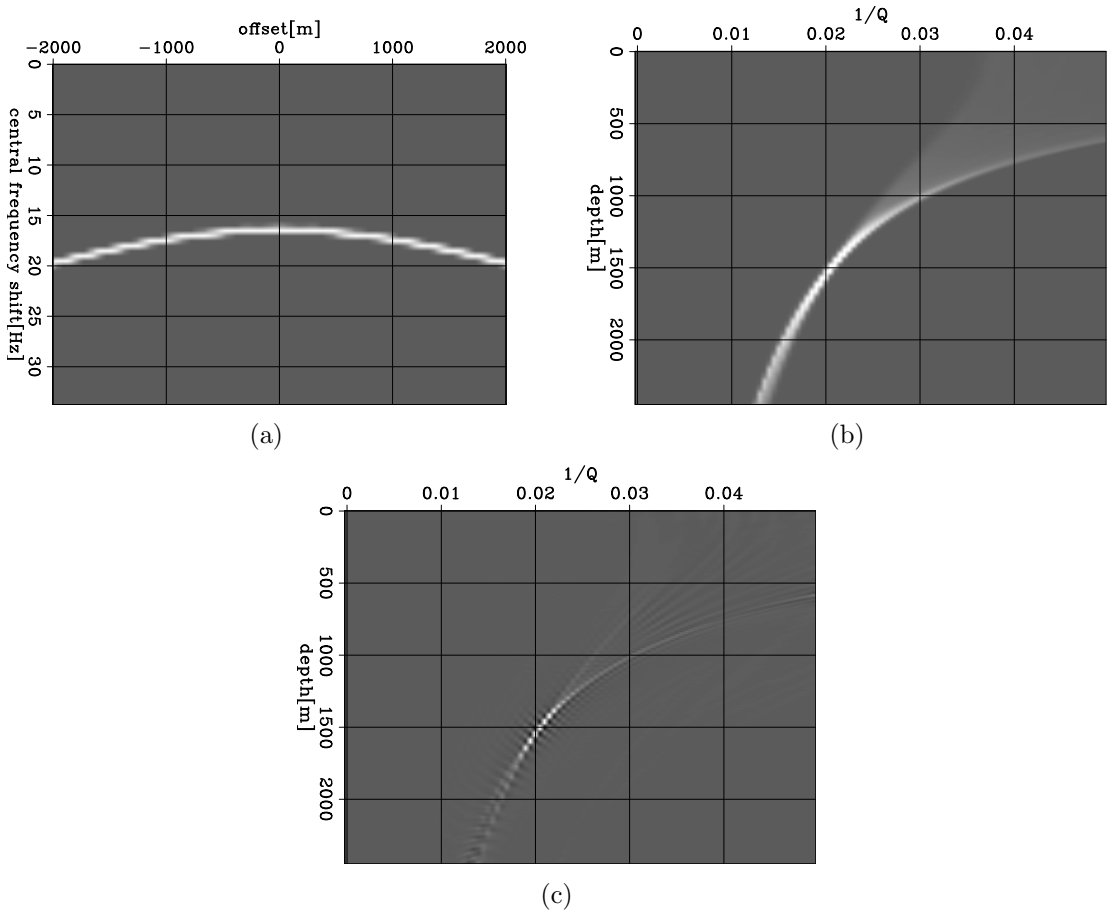

Figure 2: Figure 2(a) shows the central-frequency shift of the modeled data in Figure 1(a). The Q-spectra is computed in Figure 2(b). This result shows concentrated energy around the expected point (1500 m, 0.02), which indicates that the RMS Q is 50 above 1500 m depth. Figure 2(c) shows least-squares inversion after 50 iterations. The energy is more focused on the expected point and shows much higher resolution. [**ER**]

In reality, however, this data-domain method can be inaccurate when lateral velocity variations and dipping structures exist. Therefore, image-domain methods is needed to more accurately estimate Q.

Q migration

As with forward modeling, I use constant-Q assumption in Q migration. For convenience, I rewrite equation 9 in the form of slowness:

$$\tilde{s}(\omega) = s_{\omega r}\left(1 - \frac{1}{\pi Q}\ln(\omega/\omega_r)\right)\left(1 + \frac{i}{2Q}\right), \tag{11}$$

where $S_{\omega r}$ is the slowness at the reference frequency ω_r.

Having the new velocity/slowness, I obtain the new single square root as

$$\begin{aligned} k_z &= \mathrm{SSR}(\omega, \mathbf{k}) \\ &= \sqrt{(\omega\tilde{s})^2 - |\mathbf{k}|^2} \\ &= \sqrt{\left(\omega s_{\omega r}\left(1 - \frac{1}{\pi Q}\ln(\omega/\omega_r)\right)\left(1 + \frac{i}{2Q}\right)\right)^2 - |\mathbf{k}|^2}. \end{aligned} \tag{12}$$

This new SSR can be approximated into a simplified form by using Taylor expansion around reference slowness s_0 and reference quality factor Q_0:

$$k_z(s_{\omega r}, Q) = k_{z0}(\tilde{s}_0) + \omega\left(\tilde{s} - \tilde{s}_0\right) + \omega\left(\tilde{s} - \tilde{s}_0\right)\frac{2\,|\mathbf{k}|^2}{4\omega^2\tilde{s}_0^2 - 3\,|\mathbf{k}|^2}, \tag{13}$$

where

$$\tilde{s} = s_{\omega r}\left(1 - \frac{1}{\pi Q}\ln(\omega/\omega_r)\right)\left(1 + \frac{i}{2Q}\right), \tag{14}$$

$$\tilde{s}_0 = s_{\omega r0}\left(1 - \frac{1}{\pi Q_0}\ln(\omega/\omega_r)\right)\left(1 + \frac{i}{2Q_0}\right), \tag{15}$$

and $s_{\omega r}$ is the reference slowness at the reference frequency. The first two terms of equation 13 describe the split-step migration. The third term is the high-order correction, which allows for pseudo-screen migration.

The single square root for FFD migration is shown as follows:

$$\begin{aligned} k_z &= k_z^{\text{ref}} + k_z^{\text{split - step}} + k_z^{\text{f - d}} \\ &= (\sqrt{(\omega\tilde{s})^2 - |\mathbf{k}|^2}) + \omega\left(\tilde{s} - \tilde{s}_0\right) - \omega\tilde{s}\frac{a\left(1 - \frac{\tilde{s}_0}{\tilde{s}}\right)\left(\frac{1}{\omega\tilde{s}}\,|\mathbf{k}|\right)^2}{1 - b\left(1 + \frac{\tilde{s}_0^2}{\tilde{s}^2}\right)\left(\frac{1}{\omega\tilde{s}}\,|\mathbf{k}|\right)^2}, \end{aligned} \tag{16}$$

where $a = 0.5$ and $b = 0.25$ for 45-degree migration.

In addition, I can rewrite Q migration in a matrix form to conveniently compare with the conventional migration. The conventional migration can be written in the following matrix form:

$$\begin{aligned} \mathbf{d} &= \mathbf{F}\mathbf{m} \\ \mathbf{m} &= \mathbf{F}^T\mathbf{d} \end{aligned} \tag{17}$$

where $\mathbf{d}$ is the data, $\mathbf{m}$ is the model, $\mathbf{F}$ is the migration operator, and the superscript T indicates the matrix transpose.

The downward continuation migration with Q can be written as

$$\begin{aligned} \mathbf{d} &= \mathbf{A}\mathbf{F}\mathbf{m} \\ \mathbf{m} &= \mathbf{F}^T\mathbf{A}^T\mathbf{d}, \end{aligned} \tag{18}$$

where **A** is the attenuation operator, which consists of real numbers less than 1.

Equation 18 indicates that the migrated model will be further attenuated, with the attenuation operator **A** being applied to the attenuated modeled data. Therefore, Q migration will compensate for the phase change, but will not compensate for the amplitude loss due to attenuation.

In this section, I apply Q migration to the modeled data in Figures 1(a) and 1(b). Figure 3(a) shows the conventional migration of the non-attenuated data in Figure 1(b), which images the reflector at 1500 m depth. Figures 3(b) and 3(c) show the conventional migration and Q migration of the attenuated data in Figure 1(a). The wavelets in Figure 3(c) are stretched in comparison to the ones in Figure 3(a). This result confirms that Q migration further attenuates the data, instead of compensating for its amplitude loss.

Q compensation

In order to compensate for the amplitude loss to estimate Q in the image domain, I need Q compensation, which can be written in the following matrix form:

$$\begin{aligned} \mathbf{d} &= \mathbf{AFm} \\ \mathbf{m} &= \mathbf{F}^T\mathbf{A}^{-1}\mathbf{d}, \end{aligned} \tag{19}$$

where

$$\mathbf{A}^{-1} = \frac{\mathbf{A^T}}{\mathbf{A^T A}}. \tag{20}$$

One thing to notice is that the compensated amplitude in equation 19 contains both attenuation and an evanescent wave. However, only the attenuation part needs to be compensated. Therefore I need to remove the evanescent wave from the amplitude compensation. For a single frequency, the attenuation operator is shown as follows:

$$A = e^{-\Delta z\,\mathrm{Im}(k_z)}. \tag{21}$$

After removing the evanescent part from the amplitude compensation, the inverse attenuation operator is shown as follows:

$$A^{-1} = \frac{e^{-\Delta z\,\mathrm{Im}(k_z)}}{e^{-2\Delta z\,\mathrm{Im}(k_z - k_{Q=\infty})}}. \tag{22}$$

Figure 3(d) shows Q compensation on the attenuated data, showing exactly the same result as Figure 3(a), which has no attenuation in either forward propagation or backward imaging. This result indicates that Q compensation adequately restores the amplitude loss caused by attenuation.

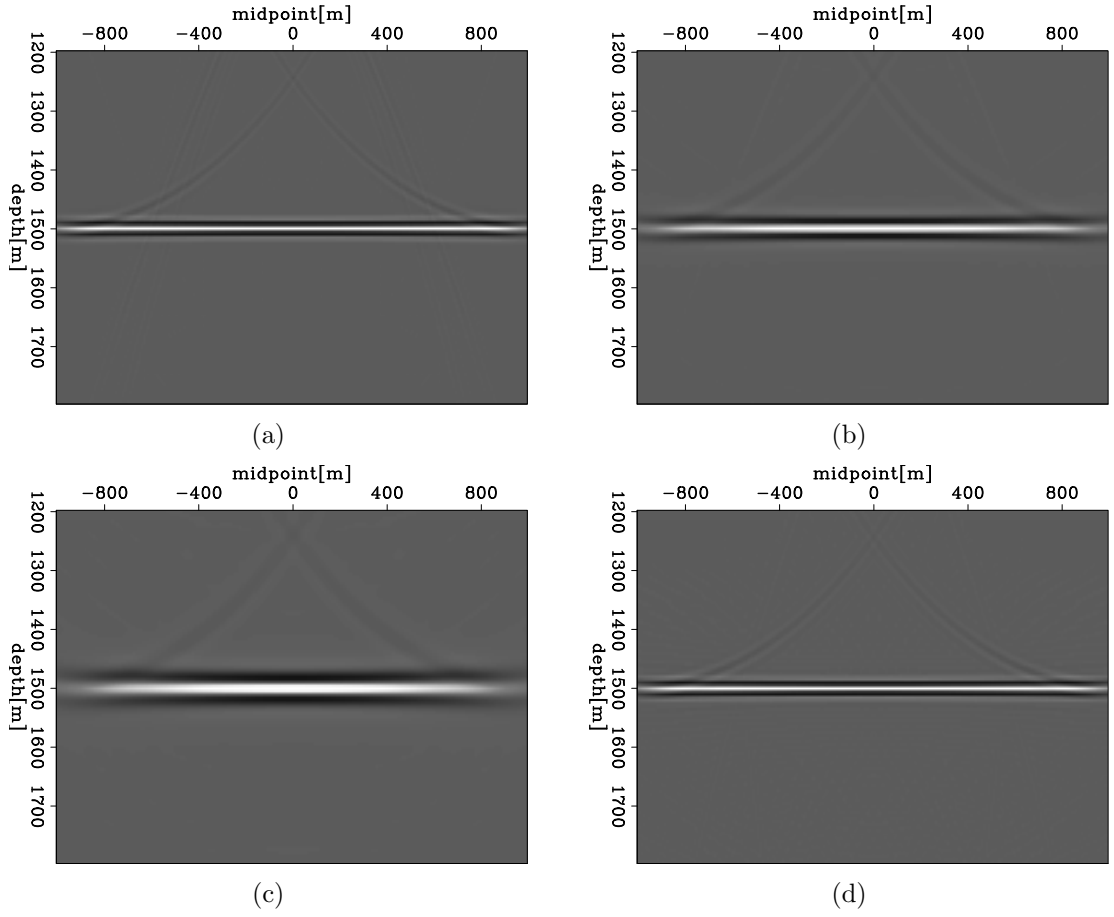

Figure 3: Given the 2D synthetic example, (a) conventional migration on non-attenuated data; (b) conventional migration on attenuated data; (c) Q migration on attenuated data; (d) Q compensation on attenuated data. [**ER**]

Estimation of Q from image space

In the presence of complex structures and/or strong lateral Q variations, extracting Q information in the data space is both inaccurate and time consuming. In these situations, the image space is a more appropriate domain for extracting kinematic information, since migration/compensation focuses and greatly simplifies the events. Even when the Q for migration/compensation is far from the true Q, the unflattened central frequency shift is a step in the right direction. I present two ways of doing this migration Q analysis (MQA).

Depth-migration Q analysis

I use the wavenumber computed from surface offset-domain common-image gathers to improve the compensation Q function by performing a moveout analysis. A straightforward procedure to update the Q function is the following:

- First, take one common midpoint to compute the image wavenumber shift in its surface offset-domain common-image gathers after depth Q compensation. Here I define the image wavenumber as $k_{\text{img}} = 2\pi f/v$, which has an angle-dependent stretch of the vertical wavenumber k_z according to the following relation: $k_{\text{img}} = k_z/2cos\theta$, where θ is the opening angle. For a flat reflector, $cos\theta = z/\sqrt{x^2+z^2}$. Substituting this defined image wavenumber into equation 10, I get the central-image wavenumber shift in the following way:

$$\Delta k = \frac{8\sigma_s^2\pi^2}{v^2}(\frac{1}{Q} - \frac{1}{Q_\rho})\sqrt{x^2+z^2}, \tag{23}$$

  where Q is the quality factor for forward modeling, Q_ρ is the quality factor for Q compensation, and $\Delta k = \frac{4\pi f_S}{v} - k_{\text{img}}$, which is defined as the central-image wavenumber shift.

  For the data generated by a flat reflector and homogeneous velocity and Q in Figures 1(a) and 1(b), images migrated or compensated using one shot at 0 m in Figure 3 is equivalent to a single image point at 0 m with respect to different source-receiver offsets. Although one shot is not enough for stacking during migration/compensation, it is still appropriate to analyze Q effect by using a limited range of the offsets.

  According to equation 23, if I plot the central-image wavenumber versus the offset or angle, the central wavenumber is flat with the correct Q for compensation, but shows a curvature with an incorrect Q for compensation. Figure 4(a) and 4(b) display the central image wavenumber of the image in Figure 3(b) and Figure 3(d). The central image wavenumber is almost flat over offsets in Figure 4(b) after being compensated with correct Q ($Q = 50$). In contract, Figure 4(a) shows a curvature along offset, since infinite Q was used for compensation. The results indicate that central-wavenumber shift is related to attenuation and can be used to estimate Q in the image domain.

The image wavenumber k_{image}, rather than the vertical wavenumber k_z, is used to relate to attenuation in this paper. The reason for not using k_z is that the central-vertical wavenumber shift is independent of the offset/angle for a simple model with a flat reflector, which can be shown as follows:

$$\Delta k_z = \frac{8\sigma_s^2\pi^2}{v^2}(\frac{1}{Q} - \frac{1}{Q_\rho}), \tag{24}$$

where $\Delta k_z = \frac{4\pi f_S}{v}\frac{z}{\sqrt{x^2+z^2}} - k_z$. Thus, the central-vertical-wavenumber shift can not be applied to QVO/QVA analysis nor to estimating Q.

- Second, an inverse shift correction is applied to the gathers, according to the RMS Q used to compensate the data. Here I describe the shift correction using the following equation:

$$(\frac{1}{QC'})^2(x^2+z^2) = \Delta k_{img}^2, \tag{25}$$

where $C' = v^2/(2\pi^2\sigma_s^2)$.

- Third, Q spectra are computed for the CIGs after the inverse shift correction. Then the RMS Q measured from the Q spectra are used to generate a new RMS-Q function. The new RMS-Q function is used to compensate the data again, and, if needed, the process can be repeated to further improve the Q value.

  Figure 4(c) shows the Q spectra of Figure 3(b) that has incorrect Q for compensation. This result shows concentrated energy around the point (1500 m, 0.02), which indicates that the new RMS-Q is 50 above 1500 m. However, the energy is not as well focused as that in Figure 2(b), because of its relatively narrow range of offsets after imaging.

CONCLUSION

I first reviewed two main methods of estimating seismic attenuation: ray-based tomography and the wave-equation-based method. Then I presented a new method for estimating Q, which uses central frequency shift to analyze Q versus offset (QVO) or Q versus angle (QVA). Based on this proposed method, I developed theories for estimation of Q in both data space and image space, and applied them to a 2D synthetic model. I also presented Q migration and Q compensation methods based on one-way wave equation. Our results showed that Q compensation recovers the amplitude loss caused by attenuation, which is a successful step forward for image-based Q estimation.

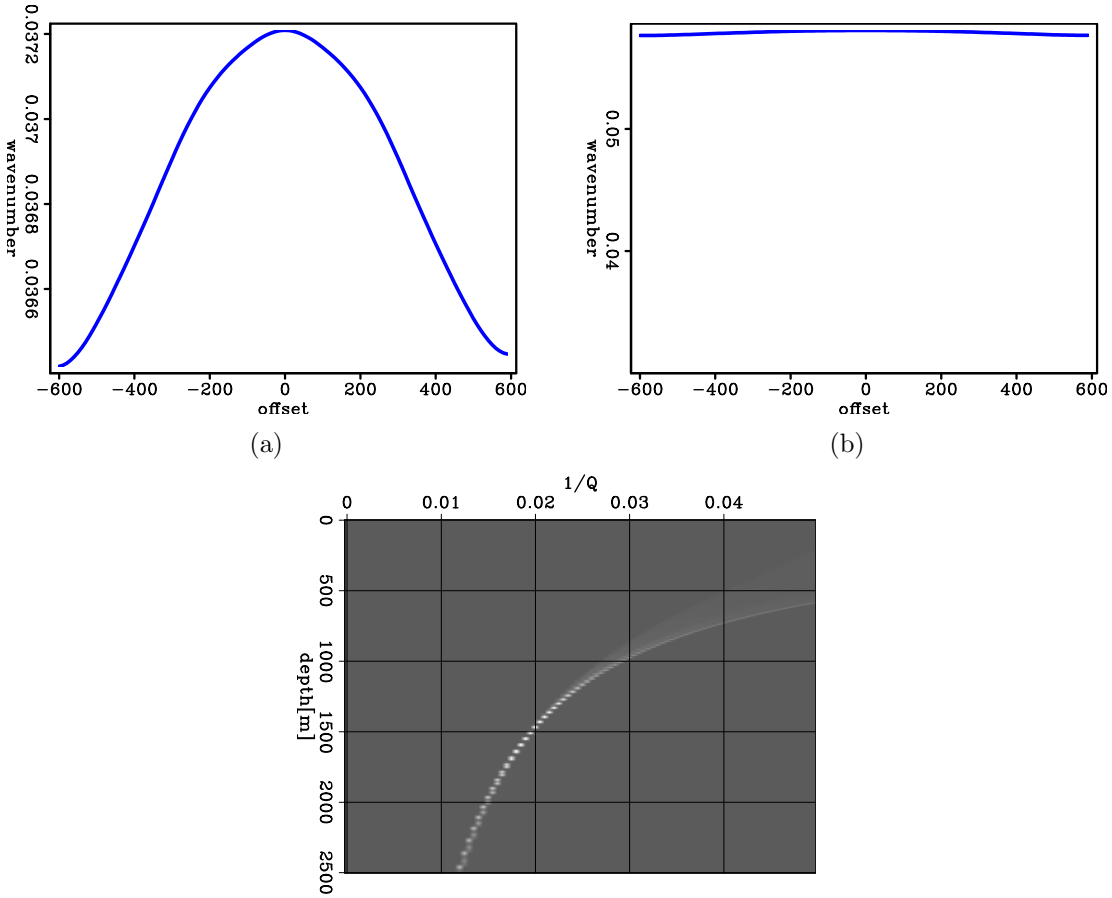

Figure 4: Given the 2D synthetic example, (a) central image wavenumber with correct Q (Q=50) for compensation ; (b) central image wavenumer with incorrect Q (Q=99999) for compensation; (c) Q spectra of Figure 3(b) that has incorrect Q for compensation. [**ER**]

FUTURE WORK

Ray-based Q-estimation methods have serious drawbacks for complex depth-imaging problems. In the presence of complex wave propagation (i.e. multipathing and geometrical dispersion), ray-based migration methods often cannot produce high-quality images, while wavefield-continuation methods yield better images. Therefore, wave-equation MQA (WEMQA) is needed to avoid the well-known instability problems that rays encounter when the Q model is complex and has sharp boundaries. The objective function of this method minimizes the residual wavenumber shift (equation 23) in the angle/offset domain. The theory and numerical results for this method are a topic of ongoing study.

ACKNOWLEDGMENTS

Thanks to Biondo Biondi, Robert Clapp and Dave Nichols of Stanford for discussions and suggestions.

REFERENCES

Blanchard, T. D., R. A. Clark, M. van der Baan, and E. Laws, 2009, Timelapse attenuation as a tool for monitoring pore fluid changes in hydrocarbon reservoirs: 71st Conference and Exhibition, EAGE, Expanded Abstracts, P052.

Clark, R. A., P. M. Benson, A. J. Carter, and C. A. G. Moreno, 2009, Anisotropic P-wave attenuation measured from a multi-azimuth surface seismic reflection survey: Geophysical Prospecting, **57**, 835–845.

Clark, R. A., A. J. Carter, P. C. Nevill, and P. M. Benson, 2001, Attenuation measurements from surface seismic data azimuthal variation and time-lapse case studies: 63rd Conference and Technical Exhibition, EAGE, Extended Abstracts, L–28.

Dasgupta, R. and R. A. Clark, 1998, Estimation of Q from surface seismic reflection data: Geophysics, **63**, 2120–2128.

Futterman, W. I., 1962, Dispersive body waves: Journal of Geophysical Research, **67**, 5279–5291.

Gao, F., G. Fradelizio, A. Levander, G. Pratt, and C. Zelt, 2005, Seismic velocity, Q, geological structure, and lithology estimation at a groundwater contamination site: 75th Annual International Meeting, SEG, Expanded Abstracts, 1561–1564.

Hackert, C. L. and J. O. Parra, 2004, Improving Q estimates from seismic reflection data using well-log-based localized spectral correction: Geophysics, **69**, 1521–1529.

Hicks, G. J. and R. G. Pratt, 2001, Reflection waveform inversion using local descent methods: Estimating attenuation and velocity over a gas-sand deposit: Geophysics, **66**, 598–612.

Liao, Q. and G. A. McMechan, 1996, Multifrequency viscoacoustic modeling and inversion: Geophysics, **61**, 1371–1378.

Moffat, L. C., R. A. Clark, M. van der Baan, and T. Manning, 2009, Azimuthal

variations of attenuation analysis applied on a 3D multiazimuth towed-streamer dataset: Research Workshop, EAGE/SEG, Expanded Abstracts, B06.

Plessix, R. E., 2006, Estimation of velocity and attenuation coefficient maps from crosswell seismic data: Geophysics, **71**, S235–S240.

Pratt, R. G., K. Bauer, and M. Weber, 2003, Crosshole waveform tomography velocity and attenuation images of Arctic gas hydrates: 73rd Annual International Meeting, SEG, Expanded Abstracts, 2255–2258.

Quan, Y. and J. M. Harris, 1997, Seismic attenuation tomography using the frequency shift method: Geophysics, **62**, 895–905.

Rickett, J., 2006, Integrated estimation of interval-attenuation profiles: Geophysics, **71**, A19–A23.

———, 2007, Estimating attenuation and the relative information content of amplitude and phase spectra: Geophysics, **72**, R19–R27.

Watanabe, T., K. T. Nihei, S. Nakagawa, and L. R. Myer, 2004, Viscoacoustic waveform inversion of transmission data for velocity and attenuation: Journal of the Acoustical Society of America, **115**, 3059–3067.

Xin, K., B. Hung, S. Birdus, and J. Sun, 2008, 3D tomographic amplitude inversion for compensating amplitude attenuation in the overburden: 78th Annual International Meeting, SEG, Expanded Abstracts, **27**, 32–39.